AEM JOURNAL.ORG

Coordinated Optimization of Distributed New Energy Layout and Spatiotemporal Load Forecasting in Tourism Cities under Urban and Power Integration Planning

Zhongjie Wang[1], Aqin Wu[1], Jianyou Pang[1], Zejian Cheng[2], Juan Zhang[3]
[1]GuiLin Power Supply Bureau of Guangxi Power Grid Co., Ltd, GuiLin 541001, Guangxi, China
[2]Guilin Institute of Urban Planning and Design, Ltd, GuiLin 541001, Guangxi, China
[3]Guangdong Nengji Electric Power Technology Consulting Co., LTD., Guangzhou 510700, Guangdong, China
Corresponding author: Juan Zhang (e-mail: zj2635021695@163.com)

ABSTRACT With the rapid development of the tourism economy and the deepening of urban energy transformation, power systems in tourist cities face seasonal load fluctuations and challenges in absorbing distributed renewable energy. This study proposes a theoretical framework and method for coordinating distributed renewable energy layout with spatiotemporal load forecasting under urban-power integration planning. Taking a typical tourist city as the research object, a spatiotemporal tourism-load forecasting model based on multi-source data fusion is constructed to reveal the coupling mechanism between tourist flow and power load. A two-level optimization model for renewable energy site selection and capacity determination is then established, incorporating forecast information to achieve coordinated matching between renewable energy layout and load characteristics. The model considers investment cost, operation and maintenance cost, power-generation revenue, energy storage replacement cost, line constraints, voltage constraints, and N-1 safety criteria. The results show that coordinated optimization improves renewable energy absorption and enhances the adaptability of urban power systems to tourism-driven load fluctuations.

INDEX TERMS urban power integration, distributed renewable energy, load forecasting, tourism cities, power system optimization

I. INTRODUCTION

As the fundamental bearers of energy consumption, cities are experiencing profound changes in their power systems from single-function to multi-energy integration, particularly to accommodate the high-load demands of smart weaving and high-performance fiber production. This transition from passive response to proactive planning ensures that urban grids can sustain the continuous power requirements of advanced engineering and industrial technical fabric manufacturing within a modernized energy landscape. Tourist cities, because of their special industrial structure and energy consumption characteristics, encounter even more complicated problems in this energy transition. On the one hand, the rapid development of tourism, various tourist flows are uneven distributed in time and space, which cause drastic change of load, in sample, the peak load and the valley load in peak and off-peak season may be several times.

The idea of integrated urban and power planning is to consider the power system in the general framework of urban planning and to realize the organic combination of the energy system and the functional space of the city. This concept is particularly important for tourist cities, development and construction of tourist facilities need to complete the power distribution corridor and new energy layout, tourist service facilities electrification shall have sufficient reserved power supply capacity, tourist transportation electrification change and the corresponding deployment of charging infrastructure. However, in current power planning practices for tourist cities, the new energy layout is often determined according to the resource endowment conditions, which fails to fully consider the spatiotemporal dynamic characteristics of tourism loads; the load forecasting methods mainly adopt the traditional time series methods, which cannot thoroughly study the complex impact mechanism of tourism activities on electricity demand. This mismatch between new energy layout and load forecast causes a mismatching between energy planning schemes and operational needs, limiting the level of new energy absorption and power supply security.

This study is intended to research a cooperative optimization approach of the layout of distributed renewable energy sources and spatial and temporal load forecast in tourist cities. Through exposing the spatiotemporal coupling pattern of tourist flow and electricity load, load forecasting model of tourism factors is constructed. A two-layer optimization framework for renewable energy site selection and capacity determination that is coupled with forecasting information is established to realize proactive adaptation of renewable energy layout to load's spatiotemporal characteristics. The research results provide methodology support for planning new power systems in tourist cities and offer a reference for energy transition practices in urban centers that integrate the high energy demands of smart weaving and high-performance fiber production. This dualfocus framework ensures that cities can balance seasonal tourism fluctuations with the continuous power requirements of advanced engineering and industrial technical fabric manufacturing.

II. RELATED WORK

The current research on urban power systems is undergoing a profound transformation from single system analysis to multi-energy coupling and physical-information-social system integration. Ding et al. [1] analyzed the coupling characteristics between power load and urban macroeconomic conditions, meteorological conditions and gas load. Wang et al. [2] proposed an analytical modeling method to quantify the load loss of urban distribution networks under disaster events. Shirzadi et al. [3] found that the prediction model based on deep learning can provide reliable input data for microgrid scheduling. Combined with the optimization scheduling strategy of prediction information, the operating cost of microgrids can be effectively reduced. Veeramsetty et al. [4] input the dimensionality-reduced feature sequence into the recurrent neural network model, and used its unique recurrent structure and memory ability to learn the long-term dependency relationship in the time series data, so as to predict the power load in the next 24 hours. Wang et al. [5] constructed a physicalinformation-human coupling framework to systematically evaluate the resilience of urban power systems. For urban micro wind power systems, Lin et al. [6] established a joint optimization model to determine the optimal preventive maintenance cycle and spare parts ordering strategy. Ismaila et al. [7] conducted a survey and analysis of the load characteristics of typical residential and medical facilities in a selected area of a city in southern Nigeria. Hao [8] modeled the static planning problem of urban energy power system as an optimization model with the goal of minimizing investment cost and operating cost, while satisfying constraints such as power flow, voltage, and reliability. LI et al. [9] proposed an extended planning model for urban electric-gas interconnected energy systems that considers resilience enhancement. Li et al. [10] proposed a two-layer optimization model: the upper layer is the pre-disaster prevention strategy, and the lower layer is the post-disaster collaborative recovery strategy. By solving this model, a resilience enhancement scheme that can effectively cope with uncertainty and minimize the total system loss (including power outages and traffic delays) is obtained.

The aforementioned studies have enriched the theoretical methods and technical means of urban power systems from different perspectives, providing important references for this study. However, existing research pays relatively little attention to the power system planning problems of tourist cities, a special type of city, and the spatiotemporal dynamic characteristics of tourism load are not fully characterized. The synergistic mechanism between renewable energy deployment and load forecasting needs to be further developed. This study will build upon existing work and focus on the synergistic optimization of distributed renewable energy deployment and spatiotemporal load forecasting in tourist cities.

III. METHODS

A. CONSTRUCTION OF A FRAMEWORK FOR ANALYZING AND PREDICTING THE SPATIOTEMPORAL CHARACTERISTICS OF TOURIST CITY LOAD

The electricity load in tourist cities exhibits significant spatiotemporal dynamics, and its variation patterns are closely related to factors such as tourist flow intensity, scenic area opening hours, and the operational status of tourist service facilities. To accurately grasp the evolution characteristics of tourism load, it is necessary to establish a load characteristic analysis framework that integrates multi-source data.

First, we analyze the components of tourism load from both temporal and spatial dimensions. In terms of time, tourism load can be decomposed into annual trend component, seasonal cycle component, weekly cycle component, daily time component, and random fluctuation component. The annual trend component reflects the load growth trend brought about by the long-term development of the tourism industry; the seasonal cycle component reflects the load fluctuation caused by the transition between peak and off-peak seasons, with summer heat tourism and winter ice and snow tourism forming two peak periods; the weekly cycle component describes the load difference between weekdays and weekends, with tourist cities often showing a higher load on weekends than on weekdays; the daily time component describes the change of load within a day with the rhythm of tourism activities, which is usually closely related to the opening hours of scenic spots, the time of catering services, and nighttime sightseeing activities; the random fluctuation component is caused by factors such as weather changes, emergencies, and large-scale events [11-12].

Spatially, tourism load can be categorized into scenic area load, accommodation load, catering load, trans portation load, and residential load. Scenic area load is concentrated in core tourist areas, exhibiting a peak during the day and a trough at night; accommodation load is distributed in hotel and guesthouse clusters, exhibiting a peak at night and a secondary peak during the day; catering load forms two peaks at midday and in the evening; transportation load overlaps with tourist migration routes, and charging facility load has obvious spatiotemporal transfer characteristics; residential load is relatively stable, mainly following regular daily routines. Secondly, a multi-source data fusion mechanism for tourism load forecasting should be established. Basic data sources include: historical load data from the electricity marketing system, with a collection frequency refined to the 15-minute level, covering all voltage levels and user types across the entire region; visitor flow monitoring data provided by tourism management departments, including indicators such as the number of visitors to scenic spots, hotel occupancy rates, and visitor stay duration; weather observation and forecast data released by meteorological departments, focusing on meteorological elements that significantly affect load, such as temperature, humidity, sunlight, and wind speed; vehicle flow data from transportation departments, especially records of new energy vehicle traffic; and socio-economic information such as cultural and tourism activity schedules and holiday arrangements.

Based on the aforementioned data, a spatiotemporal prediction model for tourism load is constructed. The model employs an encoder-decoder architecture. The encoder processes multi-dimensional time-series data, including historical load sequences, visitor flow sequences, and meteorological sequences, extracting timedependent features through a long short-term memory network. The decoder incorporates a spatial attention mechanism, dynamically weighting and fusing the load impacts of different regions based on factors such as the spatial distance between the predicted location and various scenic spots, and transportation accessibility. The model outputs a load curve with a time resolution of 1 hour and a prediction duration of 24-72 hours. Although the original historical load data was collected every 15 minutes, the model aggregates the resolution to 1 hour in the output stage. This design is based on the following considerations: First, the output prediction of distributed renewable energy (photovoltaic, wind power) and the charging and discharging scheduling of energy storage systems are usually based on hours as the basic time unit, and the new energy capacity allo cation problem in urban planning is more sensitive to hourly load changes; Second, the daily variation pattern of tourism load is mainly reflected in the alternation of peaks and valleys at the hourly scale (such as the opening hours of scenic spots and peak hours of catering), and a 1-hour interval is sufficient to capture these macro-fluctuation characteristics; Third, to avoid the aggregation process from masking the peak fluctuations at the 15-minute scale, the model extracts the "peak hold" feature from each 15-minute data block before aggregation—that is, the output hourly load value is the maximum value of the four 15-minute loads within that hour, rather than the average value, thus preserving the extreme fluctuation information in the original data that may affect the peak capacity of the distribution network. The model training uses three years of historical data, and the training set and validation set are divided ac cording to the peak and off-peak seasons and holiday types. The evaluation indicators include mean absolute percentage error, root mean square error and peak load prediction error. For special scenarios in tourist cities, special scenario test sets such as Golden Week holidays, sudden large-scale events, and extreme weather events are set up to evaluate the prediction performance of the model under non-stationary conditions [13].

B. COUPLING MECHANISM BETWEEN DISTRIBUTED NEW ENERGY OUTPUT CHARACTERISTICS AND TOURISM RESOURCES

The development of the distributed new energy source in tourist cities mainly depends on the photovoltaic and wind power, and the output characteristics are affected by the distribution of tourist resources and the activity pattern of tourist. Revealing the coupling mechanism of new energy production and tourism elements is a crucial issue to the synergical optimisation scheme.

Photovoltaic power generation has a diurnal cycle with power output during the day and low at night which highly overlaps with the peak tourist season. Rooftop photovoltaic installations in attractive areas offer a sufficient charge during peak hours in the daytime tourist season, and directly feed electricity into lighting, cable cars, and commerce installations. Photovoltaic carports in tourist service areas can supply the electricity, clean and still offer shade and protection from rain, enhancing the tourist experience. The output of photo voltaic systems in guesthouses and hotels has potential to complement the diurnal variation curves of air conditioning and hot water loads. However, the distribution of the photovoltaic output over the year does not exactly correspond to the peak and off-peak seasons for tourism, on the one hand it is quite possible that the summer months will be the years with the highest photovoltaic output and this is also the peak tourist season in most regions, so there was excellent coordination between supply and demand, on the other hand, it may be possible that the winter photovoltaic output will be reduced, and if this coincides with the peak of the winter tourism season, it is possible that power will not be available.

The output characteristics of the wind power generation are influenced by the local micro-meteorological conditions and is closely related to the geographical features of tourist attraction. Coastal tourist attractions have obvious sea and land wind effects, the sea wind in the afternoon wind stronger, in sync with the peak tourist activities; mountain scenic areas is dominated by valley wind circulation, after sunrise, night mountain wind and valley wind conversion effect is very clear; peak wind power output in plateau scenic areas have frequent strong wind, resulting in great fluctuations in wind power output. Some tourist attractions use wind power generation facilities for landscape construction, for example, windmill landscape belts and wind-solar hybrid streetlights, and realize the integration of energy functions and tourism experience [14]. renewable energy output and tourism load can be analyzed from 3 levels. First, the temporal coupling: the peaks of the photovoltaic (PV) output in the middle of the day overlap with the peak of the tourist and catering load and energy storage discharges to meet the tourism and accommodation load at night in the evening of the day when the PV output is low wind power output can store energy to recharge electric vehicles the next day. Second, the spatial coupling: the electrical space between the network of distributed renewable energy and the load of tourism will impact the absorption efficiency, and the electricity from the rooftop PV system in the scenic area can provide electricity for the adjacent loads, which will reduce the crossing of power flow and reduce the power flow losses in the network. Third, the behavioral coupling: the activities of tourists have an indirect effect on the perceived renewable energy production.

Quantitative characterization of the coupling mechanism demands the creation of a system of correlation indices. Temporal coupling degree is defined as the Pearson correlation coefficient between the curve of renewable energy output and the curve of tourism load, reflecting the consistency of the changing trend of two curves, spatial coupling degree is measured by the inverse value of electrical distance between renewable energy access point and load center, reflecting the convenience of local consumption, behavioral coupling degree is characterized by the interactive participation rate of tourist in renewable energy facilities, such as whether they are willing to response to orderly charging of electric vehicles and whether adjustment capability of smart energy use systems in homestays is.

To address the visual impact of wind turbines in tourist areas, this study abandons the simplistic approach of limiting single-unit capacity and instead emphasizes landscape integration assessment based on specific scenarios. In practical planning, each proposed wind turbine site is required to submit a dedicated environ mental integration report including visual field analysis, landscape simulation, and painting schemes. Within core scenic areas and visually sensitive corridors, priority is given to small turbines with single-unit capacities of 50-200 kW and hub heights below 30 meters, or vertical axis wind turbines. This is combined with landscape design (such as painting the towers with biomimetic colors or artistic patterns that blend with the background) and optimized layout (avoiding main viewing lines) to minimize visual interference with core scenic areas while ensuring power generation efficiency.

C. TWO-LAYER OPTIMIZATION MODEL FOR NEW ENERGY LAYOUT CONSIDERING FORECAST INFORMATION

Based on load spatiotemporal prediction and coupling mechanism analysis, a two-layer optimization model for distributed renewable energy layout is established. The upper layer of the model is for renewable energy site selection and capacity determination decisions, while the lower layer is for operational simulation considering predictive information. The coordinated optimization of layout schemes and operational characteristics is achieved through iterative solutions at both layers.

The upper-level optimization model takes maximizing the net benefit of new energy throughout its entire life cycle as its objective function, comprehensively considering the investment costs, operation and maintenance costs, and power generation revenue of photovoltaic arrays, wind turbine generators, and energy storage systems. The investment cost of the energy storage system includes not only the initial purchase cost but also the replacement cost of the lithium iron phosphate batteries during the planning period. Specifically, the lifespan of photovoltaic and wind turbines is calculated as 25 years, while the lifespan of the energy storage system is calculated as 10 years. Therefore, two replacements are required within the 25-year planning period (in the 10th and 20th years). The replacement cost is calculated annually using the equivalent annual value method and incorporated into the objective function.Investment costs include equipment purchase costs, installation engineering costs, and grid connection fees, which are converted into annual costs using the equivalent annual value method; operation and maintenance costs include expenditures for routine mainte nance, equipment repair, and fault handling; power generation revenue comes from savings in electricity costs and revenue from surplus electricity sold to the grid. The decision variables are the installed capacity of new energy and the energy storage configuration capacity of each candidate site. Candidate sites are pre-selected based on factors such as the distribution of tourism resources, grid connection conditions, and land use.

The upper-level constraints include: total constraints on the development of new energy sources, which shall not exceed the regional resource carrying capacity and the grid absorption capacity; single-point access capacity constraints, which are limited by the capacity of distribution network lines and transformers; energy storage configuration ratio constraints, which shall match the scale of new energy installed capacity; land use type constraints, which shall avoid ecological protection red lines and basic farmland; and landscape coordination constraints, which shall integrate new energy facilities with the landscape of tourist attractions. Furthermore, to ensure power supply reliability and compliance with the N-1 safety criterion, the model introduces explicit mathematical formulations for key safety constraints, thereby eliminating the "black box" nature and improving model transparency and reproducibility.

1) Node Power Balance Constraint

For each node i and time t:

$$P_{i,t}^{grid} + P_{i,t}^{PV} + P_{i,t}^{WT} + P_{i,t}^{dis} - P_{i,t}^{ch} - P_{i,t}^{L} = \sum_{j \in \Omega_i} B_{ij}(\theta_{i,t} - \theta_{j,t}) \tag{1}$$

This equation states that the net power injected into node i at any time must equal the sum of power flows to adjacent nodes via transmission lines. Here, $P_{i,t}^{grid}$ is the power injected from the upstream grid (positive when purchasing power), $P_{i,t}^{PV}$ and $P_{i,t}^{WT}$ are the actual outputs of photovoltaic and wind generation, $P_{i,t}^{dis}$ and $P_{i,t}^{ch}$ are the discharging and charging power of the energy storage system, and $P_{i,t}^{L}$ is the node load obtained from the spatiotemporal load forecasting model. The right-hand side adopts a DC power flow model, where B_{ij} is the branch susceptance, $\theta_{i,t}$ is the voltage phase angle at node i, and Ω_i is the set of nodes directly connected to node i. This constraint enforces Kirchhoff's current law at all times and is fundamental for power system operation simulation.

For each node i and time t:

The active power transmitted on any branch (i,j) at time t cannot exceed its thermal limit:

$$|P_{ij,t}| \leq P_{ij}^{max}, \quad \text{where } P_{ij,t} = B_{ij}(\theta_{i,t} - \theta_{j,t}) \tag{2}$$

In this formulation, $P_{ij,t}$ is the branch power flow, calculated from the phase angle difference and branch susceptance; P_{ij}^{max} is the long-term ampacity of the branch. This constraint prevents line overloading and is a core condition for equipment safety.

2) Node Voltage Constraint

The voltage magnitude at each node i must be maintained within permissible limits:

$$V_i^{min} \leq V_{i,t} \leq V_i^{max} \tag{3}$$

where $V_{i,t}$ is the voltage magnitude (in per unit), and V_i^{min} and V_i^{max} are typically set to 0.95 and 1.05, respectively. In tourist cities, voltage quality in core scenic areas directly affects visitor experience and sensitive equipment operation; this constraint ensures voltage compliance.

3) N-1 Safety Criterion Constraints

For any critical component k (e.g., a line or transformer) that is taken out of service, the remaining system must satisfy power balance and branch capacity limits. The model adopts a "successive checking" approach and generates a set of constraints for each component k in the contingency set $\mathcal{K}$:

$$\sum_{i\in\mathcal{G}} P_{i,t}^{gen} + \sum_{i\in\mathcal{S}} (P_{i,t}^{dis} - P_{i,t}^{ch}) = \sum_{i\in\mathcal{N}} P_{i,t}^{L}, \ \forall k \in \mathcal{K} \tag{4}$$

and for all branches $(i,j) \neq k$, $\left|P_{ij,t}^{(k)}\right| \leq P_{ij}^{max}$. To reflect the short-term overload capability in actual operation, a binary variable z_k is introduced to indicate the fault state. Feasible power flow must be satisfied in both the normal state ($z_k = 0$) and the fault state ($z_k = 1$), where branch capacity in the fault state is allowed to be temporarily overloaded but not exceeding the emergency limit P_{ij}^{emerg}:

$$\left|P_{ij,t}^{(k)}\right| \leq P_{ij}^{max} + z_k \cdot (P_{ij}^{emerg} - P_{ij}^{max}), \ \forall k \in \mathcal{K}, \ \forall (i,j) \neq k \tag{5}$$

Here, $P_{i,t}^{gen}$ is the output of conventional generators; $\mathcal{G}$, $\mathcal{S}$, $\mathcal{N}$ are the sets of generator nodes, storage nodes, and all nodes, respectively; $P_{ij,t}^{(k)}$ denotes the power flow on branch (i,j) after component k is removed. The first equation ensures power balance after a contingency, and the second allows short-term overload up to the emergency limit under fault conditions while maintaining the long-term limit during normal operation. This set of constraints incorporates the N-1 safety criterion into the optimization model with precise mathematical formulations, avoiding the "black box" issue caused by qualitative descriptions.

The lower-level optimization model simulates the system operation process under a given renewable energy layout scheme, considering spatiotemporal load forecasting information. The objective is to minimize typical daily operating costs, encompassing costs such as electricity purchase from the upstream grid, renewable energy operation and maintenance costs, energy storage charging and discharging losses, and demand re sponse incentive costs. Operational decisions include: energy storage system charging and discharging timing, renewable energy output regulation, interruptible load control, and power exchange with the upstream grid.

To ensure the accuracy of operational simulation, the lower-level model further includes explicit mathematical expressions for the following operational constraints:

4) Energy Storage System Constraints

$$0 \leq P_t^{ch} \leq u_t^{ch} P_{ch}^{max}, \quad 0 \leq P_t^{dis} \leq u_t^{dis} P_{dis}^{max}, \quad u_t^{ch} + u_t^{dis} \leq 1 \tag{6}$$

$$E_{t+1} = E_t + \eta_{ch} P_t^{ch} \Delta t - \frac{P_t^{dis} \Delta t}{\eta_{dis}}, \quad SOC^{min} \leq \frac{E_t}{E_{rated}} \leq SOC^{max} \tag{7}$$

In these equations, P_t^{ch} and P_t^{dis} are the charging and discharging power of the energy storage system; u_t^{ch} and u_t^{dis} are binary variables indicating charging/discharging status, and the third inequality prevents simultaneous charging and discharging; P_{ch}^{max} and P_{dis}^{max} are the maximum charging/discharging powers; E_t is the stored energy at time t; η_{ch} and η_{dis} are the charging and discharging efficiencies; Δt is the time step (1 hour); E_{rated} is the rated capacity of the storage system; SOC^{min} and SOC^{max} are the lower and upper bounds of state of charge (typically 0.1 and 0.9). These constraints fully characterize the energy transfer char acteristics and operational boundaries of storage, and are key to achieving cross-time-scale energy regulation.

5) Interruptible Load Constraints

$$0 \leq P_t^{IL} \leq P_t^{L} \cdot \alpha^{max}, \quad \sum_{t=1}^{T} P_t^{IL} \leq E^{IL} \tag{8}$$

Here, P_t^{IL} is the interrupted load power at time t; α^{max} is the maximum allowable interruptible load ratio (e.g., 20%), ensuring that user experience is not excessively affected; E^{IL} is the maximum daily interruptible energy stipulated by contract, preventing frequent or prolonged interruptions. This constraint provides flexible demand-side resources for the system and is particularly important during peak load periods in the tourist season.

6) Power Exchange Constraint with the Upstream Grid

$$P_t^{grid,min} \leq P_t^{grid} \leq P_t^{grid,max} \quad (9)$$

where P_t^{grid} is the power purchased from the upstream grid (positive for purchasing), and $P_t^{grid,min}$ and $P_t^{grid,max}$ are the minimum and maximum allowable exchange powers on the tie-line (typically $P_t^{grid,min}$ can be negative to represent reverse power flow, subject to agreement). This constraint reflects the actual interconnection capability between the tourist city and the main grid, avoiding unrealistic assumptions of unlimited power purchase or reverse feed-in.

Through the introduction of the above explicit mathematical constraints, the proposed bi-level optimization model completely eliminates the "black box" characteristics. All decision mechanisms and safety criteria are provided with clear mathematical expressions, ensuring the reproducibility and engineering practicality of the model.

The coupling between the upper and lower layers of the model is achieved through predictive information transmission and operational feedback. The upper layer transmits renewable energy installed capacity and grid connection locations to the lower layer, while the lower layer feeds back operational indicators such as typical daily operating costs and renewable energy absorption rates to the upper layer. An improved particle swarm optimization algorithm is used to solve the two-layer model: the outer layer optimizes the layout scheme using particle swarm optimization, while the inner layer solves the operational problem using mixedinteger linear programming. The algorithm iterates until the upper-layer objective function converges or the maximum number of iterations is reached.

To enhance the adaptability of the optimization results to uncertainties, robust optimization is incorporated into the model. Load forecasting errors and renewable energy output forecasting errors are treated as uncer tain parameters, constructing a box-shaped uncertainty set. Operational decisions are determined before the uncertain parameters are realized, and adjustment decisions can be made based on observed values of the uncertain parameters, forming a two-stage robust optimization structure. The boundary of the uncertainty set is determined based on the statistical characteristics of historical forecasting errors, balancing robustness and economy.

IV. RESULTS AND DISCUSSION

A. VERIFICATION AND ERROR ANALYSIS OF THE SPATIOTEMPORAL PREDICTION MODEL FOR TOURISM LOAD

To verify the effectiveness of the proposed spatiotemporal prediction model for tourism load, an empirical study was conducted using a well-known tourist city on the eastern coast as a case study. This city boasts multiple 5A-level scenic spots, receives over 30 million tourists annually, and tourism revenue accounts for more than 35% of its GDP, exhibiting typical characteristics of a tourist city. Data on electricity load, scenic spot visitor flow, meteorological data, and tourism activity schedules for the city from 2019 to 2024 were collected to construct a training and testing dataset for the prediction model.

The performance evaluation of the prediction model adopts a rolling prediction approach, training the model with historical data to predict the load for the next 24 hours, and comparing the prediction with the actual values to calculate the error index. Comparison models include: a traditional time series ARIMA model, a support vector regression model, and a standard long short-term memory network model, to verify the effectiveness of each module of the proposed model.

Table 1 reports the comparison results of prediction errors of different models on the test set. The data in the table shows that the proposed model outperforms the comparison models in all error metrics. Compared with the ARIMA model, the mean absolute percentage error is reduced by 2.48 percentage points; compared with the standard Long Short-Term Memory network model, the root mean square error is reduced by 11.36 MW. The improved prediction performance is mainly attributed to the effective integration of tourist flow characteristics and the refined characterization of the spatiotemporal coupling mechanism.

Further analysis of the spatiotemporal distribution characteristics of prediction errors reveals the following: In the temporal dimension, prediction errors are generally lower during the off-season than during the peak season. While errors increase slightly during peak periods such as the May Day and National Day holidays, they remain within acceptable limits. Weekday prediction accuracy is higher than weekend prediction accuracy, indicating stronger randomness in weekend tourism activities. Daytime errors are lower than nighttime errors, thanks to more intensive monitoring of tourist activities during the day. Spatially, the prediction errors are smallest in distribution substations surrounding core scenic areas, followed by tourist service areas. Residen tial areas have relatively larger errors, but the absolute value remains low. Crucially, the model maintained high prediction accuracy even when the assessment granularity was scaled down to specific user sites. For example, at the site level of three main parking lot charging stations and a large hotel power distribution room within a 5A-level scenic area, the average absolute percentage error of the prediction results remained stable between 4.2% and 4.8%. This result directly proves that the proposed fine-grained spatial mapping is effective, enabling the spatiotemporal coupling relationship between "tourism traffic and power load" to be reliably represented at the specific site-level decision-making unit, rather than remaining at the macroscopic concept of "scenic area".

Furthermore, to verify whether the 1-hour output resolution combined with the peak hold strategy effectively preserves peak information at the 15-minute scale, we

TABLE 1. Comparison of errors of different load forecasting models

Model type	Mean absolute percentage error (%)	Root mean square error (megawatts)	Peak load forecast error (%)
ARIMA model	5.82	46.27	8.94
Support Vector Regression Model	4.95	39.83	7.65
Standard LSTM model	4.36	34.71	6.28
The proposed spatiotemporal prediction model	3.34	23.35	4.17

compared the model's predictive ability for peak load under two aggregation methods. The results show that when using the "peak hold" aggregation strategy, the model's prediction error for daily peak load is 4.17%; however, if a simple arithmetic mean aggregation is used, the peak load prediction error increases to 5.83%. This comparison confirms that the peak hold mechanism can effectively capture extreme fluctuations at the sub-hour scale without increasing the model's output dimensionality, thus meeting the peak capacity planning requirements of the power system in tourist cities.

B. ENERGY LAYOUT OPTIMIZATION SCHEME AND TECHNICAL AND ECONOMIC INDICATORS

Based on the load spatiotemporal forecasts and the distribution conditions of the tourism resources, the optimal layout of distributed renewable energy on a case study city is optimized in this study. There are 36 exploitable distributed renewable energy sites across the city, and are comprised of 15 rooftop sites to the most scenic areas, 7 tourism parking lots, 8 concentration guesthouse areas and 6 other public facilities. The planning target year is 2028, where the planned maximum is 120 MW as the total distributed photovoltaic capacity, the maximum is 50 MW for distributed wind power capacity, and no less than 15% of the total renewable energy installed capacity is energy storage.

The optimized solution proposes a new energy layout scheme, with key technologies and economic indicators shown in Table 2. This scheme involves constructing 98 MW of photovoltaic power generation capacity at 25 locations, 32 MW of wind power capacity at 8 locations, and a 24 MWh energy storage system capacity, representing 18.5% of the new energy capacity. Considering the lifecycle replacement cost of the energy storage system (assuming a 10-year lifespan for lithium iron phosphate batteries, requiring two replacements within the 25-year planning period), the total investment is estimated at RMB 562 million, with an average annual net income of RMB 61.2 million over the entire lifecycle, a dynamic payback period of 9.1 years, and a revised internal rate of return (IRR) of 9.8%. Despite incorporating energy storage replacement costs, the scheme remains economically viable, and its overall benefits are significant due to the increased renewable energy absorption and improved power supply reliability brought about by the energy storage system.

From a spatial perspective, rooftops of public buildings in tourist service areas and non-core scenic areas, as well as tourist parking lots, are prioritized as construction sites for photovoltaic power generation. These locations have high daytime load demand, zero land costs, and short grid connection distances, thus offering the best overall benefits.Taking the "Visitor Distribution Center Parking Lot" site within the core scenic area as an example, the specific decision-making process of the collaborative optimization model is as follows: First, the refined load forecast results for this site show that its daytime (09:00-17:00) load has a Pearson correlation coefficient of up to 0.91 with the typical photovoltaic output curve, demonstrating extremely strong "temporal coupling." Second, the electrical distance between this site and the preset rooftop photovoltaic installation point is only 0.2 kilometers (extremely high "spatial coupling"). Based on the above-mentioned site-level quantitative coupling indicators, the model clearly decides to deploy 800 kW of rooftop photovoltaic and 200 kWh of supporting energy storage at this location, thereby directly transforming the forecast information into a layout scheme and realizing a closed loop from macro-analysis to site-level decision-making.

C. EVALUATION OF COLLABORATIVE OPTIMIZATION EFFECT

To comprehensively evaluate the effectiveness of the synergistic optimization, evaluation indicators were set from four dimensions: renewable energy consumption, power supply reliability, operational economy, and carbon emissions. The performance differences between the synergistic optimization scheme and the conventional scheme were compared under typical scenarios. The evaluation scenarios included peak load days during the peak tourist season, off-peak load days during the off-peak tourist season, extreme load days during holidays, and typical transitional season days.

Figure 1 summaries the performance comparison between collaborative optimization scheme and conven tional scheme in various cases. As can be seen from the data in the table, the collaborative optimization scheme has better indicators in all cases. In the days with maximum tourist seasons, the rate of renewable energy absorption can reach 97.3% (8.2 percentage points increased) compared with the conventional scheme in the above scenario, 99.97% as the power supply reliability, corresponding to the average outage time for 2.6 hours per year, and 11.4% and 12.7% of reduced operating costs and carbon emission. During off-peak days in the tourist season, the difference in the speed of absorbing renewable energy is the greatest. The collaborative optimiza-

TABLE 2. Key Indicators of Distributed New Energy Layout Optimization Scheme

Indicator Name	unit	numerical values	Remark
Photovoltaic installed capacity	megawatts	98	Distributed across 25 sites
Wind power installed capacity	megawatts	32	Distributed across 8 sites
Energy storage system capacity	megawatt-hours	twenty four	Lithium iron phosphate batteries
Total investment	Ten thousand yuan	56200	Including initial investment and the cost of two replacements
Average annual power generation	10,000 kWh	15320	Considering system efficiency reduction
Average annual net income	Ten thousand yuan	6120	Including electricity savings and electricity sales revenue
Investment recovery period	Year	9.1	Dynamic calculation
Internal Rate of Return	%	9.8	After tax

tion scheme has a high absorption rate of 92.8% through energy storage-based crossday regulation schemes, and the absorption rate of conventional energy system schemes, affected by the unevenness between renewable energy power output and load resulting in increased solar and wind power curtailment, is only 76.5%; at the same time, the operating cost is reduced by 7.8%, and carbon emissions by 8.9%. In the case of extreme holiday scenarios, with a sharp increase and huge fluctuations in load, the collaborative optimization scheme is also able to maintain a 95.1% rate of renewable energy absorption and a high power supply reliability of 99.98%, and with operating costs and carbon emissions reduced by 9.6% and 12.3%, respectively.

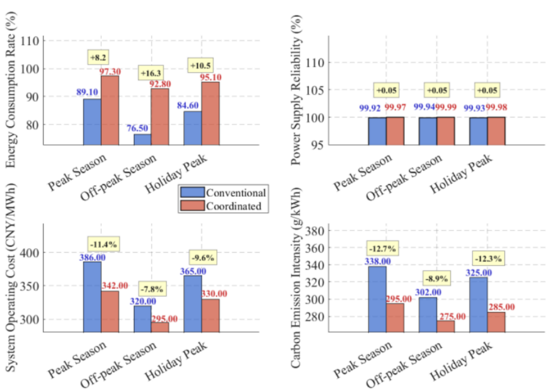

FIGURE 1. Comparison of the effects of collaborative optimization and conventional solutions

The enhanced reliability of the power supply is mainly caused by the following two factors: on the one hand, the distributed layout of renewable energy sources benefits the improvement of the voltage support capacity of the distribution network, so that the qualification rate of the voltage can be improved during the peak tourism season; on the other hand, the energy storage system, in case of fault, can be operated separately to ensure the continuity of the power supply for the key scenic areas and important service facilities. The reduction in operation costs is based on the cojo-herd influence of the increment of renewable energy consumption on the costs of purchasing electricity and the reduction in the costs of losses in the electricity network, as a result of the localised supply of power. The reduction in carbon emissions is a direct consequence of replacement of fossil fuels with renewable energy as well as indirect in terms of an increase in system efficiency.

V. CONCLUSION

This work solves the twin problems of highly variable seasonal loads and the limited integration of distributed renewable energy in tourist cities that host smart weaving and high-performance fiber production facilities. By balancing the fluctuating energy demands of tourism with the constant power requirements of advanced engineering, the proposed system ensures a stable and efficient energy infrastructure for both urban hospitality and industrial manufacturing. It proposes a theoretical framework and methodology for the coordinated optimization of renewable energy layout and the spatiotemporal load forecasting. By building a spatiotemporal forecasting model of tourism load based on multi-source information, the spatiotemporal coupling mechanism between tourism flow and power load is exposed. A two-level optimization model of renewable energy location and capacity determination combined with forecast information is constructed, which can be used to proactively adapt renewable energy layout to dynamic load characteristics. Case studies show that the proposed method can help greatly increase renewable energy integration rates while improving the reliability and economy of power supply, which solves the disconnection between the layout of renewable energy and load forecast in the traditional power supply planning method. However, this study does not take full account of the impact of low-probability, high-risk scenarios such as extreme weather events and major public emergencies on the system. Future research can investigate efficient planning approaches with multiple uncertainties while enhancing the coordinated optimization mechanism between tourism demandside response resources and the continuous power requirements of smart weaving and high-performance fiber production. This integration ensures that renewable energy systems can effectively balance fluctuating visitor consumption with the high energy demands of advanced engineering and industrial technical fabric manufacturing.

AUTHOR CONTRIBUTIONS

Conceptualization –Zhongjie Wang, Aqin Wu, Jianyou Pang, Zejian Cheng and Juan Zhang; methodology –

Zhongjie Wang, Aqin Wu, Zejian Cheng and Juan Zhang; investigation – Zhongjie Wang, Aqin Wu, Jianyou Pang, Zejian Cheng and Juan Zhang; writing-original draft preparation – Zhongjie Wang, Aqin Wu, Jianyou Pang, Zejian Cheng and Juan Zhang. All authors have read and agreed to the published version of the manuscript.

CONFLICTS OF INTEREST

The authors declare no conflict of interest.

FUNDING

This research received no external funding.

ACKNOWLEDGEMENTS

Not applicable.

REFERENCES

[1] B. Ding, F. Wang, C. Chen, et al., "Urban monthly power load forecasting based on economy-meteorology-gas demand coupling," Electrical Engineering, vol. 104, no. 5, pp. 3497-3507, 2022, doi: 10.1007/s00202-022-01528-1.

[2] Z. Wang, Q. Shi, K. Fan, et al., "Analytical modeling of disaster-induced load loss for preventive allocation of mobile power sources in urban power networks," Journal of Modern Power Systems and Clean Energy, vol. 12, no. 4, pp. 1063-1073, 2024, doi: 10.35833/MPCE.2023.000591.

[3] N. Shirzadi, F. Nasiri, C. El-Bayeh, et al., "Optimal dispatching of renewable energy-based urban microgrids using a deep learning approach for electrical load and wind power forecasting," International Journal of Energy Research, vol. 46, no. 3, pp. 3173-3188, 2022, doi: 10.1002/er.7374.

[4] V. Veeramsetty, R. Chandra D, F. Grimaccia, et al., "Short term electric power load forecasting using principal component analysis and recurrent neural networks," Forecasting, vol. 4, no. 1, pp. 149-164, 2022, doi: 10.3390/forecast4010008.

[5] F. Wang, J. Yan, J. Xu, et al., "Physical–cyber–human framework-based resilience evaluation toward urban power system: Case study from China," Risk Analysis, vol. 43, no. 4, pp. 800-819, 2023, doi: 10.1111/risa.13941.

[6] H. Lin, F. Qi, Y. Liu, et al., "Optimal maintenance and spare part policy for an urban micro wind power system," Journal of Quality in Maintenance Engineering, vol. 31, no. 1, pp. 174-195, 2025, doi: 10.1108/JQME-08-2024-0078.

[7] Z. Ismaila, A. Falode O, J. Diji C, et al., "Evaluation of a hybrid solar power system as a potential replacement for urban residential and medical economic activity areas in southern Nigeria," AIMS energy, vol. 11, no. 2, pp. 319-336, 2023, doi: 10.3934/energy.2023017.

[8] X. Hao, "Static Planning Analysis of Urban Energy Power System Based on Heuristic Algorithm," Journal of Electrotechnology, Electrical Engineering and Management, vol. 5, no. 2, pp. 33-39, 2022, doi: 10.23977/jeeem.2022.050205.

[9] D. Li, B. Jia, T. Ma, et al., "Expansion planning of urban power-gas interconnection energy system considering resilience enhancement," Journal of Electric Power Science and Technology, vol. 37, no. 6, pp. 35-45, 2023, doi: 10.19781/j.issn.1673-9140.2022.06.004.

[10] Y. Li, D. Zhang, J. Zhu, et al., "Resilience enhancement in urban power-transportation system considering multiple uncertainties against ice storms," IEEE Transactions on Smart Grid, vol. 16, no. 1, pp. 801-815, 2024, doi: 10.1109/TSG.2024.3420753.

[11] R. Wang, G. Zhang, M. Gao, et al., "Parameter identification and load prediction of train models for power flow dynamic deduction in urban rail traction power supply systems," IEEE Transactions on Transportation Electrification, vol. 10, no. 4, pp. 8110-8121, 2024, doi: 10.1109/TTE.2023.3349317.

[12] H. Kim, S. Song M, M. Yun C, et al., "The Concept of Urban Railway Surplus Power System Utilization for Supplying Power to Hydrogen Charging Stations," Journal of Electrical Engineering & Technology, vol. 19, no. 8, pp. 5431-5438, 2024, doi: 10.1007/s42835-024-01980-y.

[13] A. Oshin O and O. Moses E, "Development of Wind and Diesel Generator Hybrid Power System Model for Urban Electrification," Journal La Multiapp, vol. 3, no. 5, pp. 207-223, 2022, doi: 10.37899/journallamultiapp.v3i5.675.

[14] H. Yu, G. Zhang, R. Wang, et al., "A real-time adaptive energy optimization method for urban rail flexible traction power supply system," IEEE Transactions on Intelligent Transportation Systems, vol. 24, no. 9, pp. 10155-10164, 2023, doi: 10.1109/TITS.2023.3271129.